Temperature and Orientation Induced Polymorphic Behavior of Syndiotactic Polypropylene

ARTICLE *in* MACROMOLECULES · SEPTEMBER 2005

Impact Factor: 5.8 · DOI: 10.1021/ma050397x

2 AUTHORS:

Liberata Guadagno
Università degli Studi di Salerno
112 PUBLICATIONS **1,254** CITATIONS
SEE PROFILE

Carlo Naddeo
Università degli Studi di Salerno
53 PUBLICATIONS **656** CITATIONS
SEE PROFILE

Temperature and Orientation Induced Polymorphic Behavior of Syndiotactic Polypropylene

Liberata Guadagno,* Carlo Naddeo, and Vittoria Vittoria

Dipartimento di Ingegneria Chimica e Alimentare, Università di Salerno, Via Don Melillo 1, 84084 Fisciano, Salerno, Italy

Stefano Valdo Meille

Dipartimento di Chimica, Materiali ed Ingegneria Chimica "G. Natta" Politecnico di Milano Via Mancinelli, 7 20131 Milano, Italy

Received February 24, 2005; Revised Manuscript Received August 9, 2005

ABSTRACT: Syndiotactic polypropylene (sPP) was rapidly quenched from the melt to room temperature, obtaining films in the disordered form I, with the chains in helical conformation. A significant portion of chains in the trans-planar mesophase was found, as evidenced by X-ray diffraction and FTIR spectroscopy. The quenched films were drawn to a draw ratio of 6 at 25, 60, and 90 °C and analyzed before and after releasing the tension. A large shrinkage was observed unhooking the fibers, and this parameter, expressed as $(l_{max} - l_f)/l_{max}$, almost linearly decreased on increasing the drawing temperature. The crystalline phase composition was investigated by diffraction techniques in both the fixed and relaxed fibers. The fully extended fibers drawn at all the investigated temperatures contain a significant amount of the trans-planar mesophase while the fraction of the crystalline trans-planar form III decreases on increasing the drawing temperature and it is absent in the fiber drawn at 90 °C. Upon relaxation, we found evidence that the trans-planar mesophase in the fixed fiber crystallizes into form II while form III in the fixed fibers tends to transform into the trans-planar mesophase. An infrared and dynamic-mechanical analysis on the fibers was also performed to confirm the structural results. The analysis evidenced that on increasing the drawing temperature, the mesophase in the fixed fibers more and more transforms into the helical form II. On the other hand trans-planar chains remain in the amorphous fraction of all the relaxed fibers. The experimental results allow one to better clarify the role of the trans-planar mesophase in phase transitions of sPP and, taking into account also literature data, to propose a more detailed scheme of transformations between different polymorphs of this polymer.

Introduction

The complex polymorphism of syndiotactic polypropylene (sPP) is currently actively being investigated, mainly to clarify the transformations between different polymorphs taking place due to strain, pressure, temperature, and solvent treatments. In fact, each of these parameters strongly influences the crystallization behavior, the morphology, and the physical properties of syndiotactic polypropylene. The picture is however hardly coherent and clear because of the complexity of a polymorphic behavior involving different chain conformations and packing modes presenting closely similar internal energy values.

Four crystalline forms of sPP have been described so far, characterized either by different chain conformations or different crystal packing. In forms I and II chains adopt the $(T_2G_2)_n$ helical conformation,[1−4] whereas forms III and IV present chains in trans-planar and $(T_6G_2T_2G_2)_n$ conformations,[5−6] respectively.

Form I is the stable form of sPP. It is obtained under the most common crystallization conditions both from the melt and from solution as single crystals.[1,7,8] In this form, the helical chains are packed, in the limit-ordered structure (form I), with an alternation of right-handed and left-handed helices along both axes of the unit cell, which is orthorhombic (*Ibca*) with axes $a = 14.50$ Å, $b = 11.20$ Å, and $c = 7.45$ Å. Samples crystallized from the melt at low temperatures present disorder in this regular alternation, with an orthorhombic lattice where a and c remain the same and b is halved.

Form II corresponds to a C-centered structure in which the helical chains share the same chirality. Formerly it was obtained only by stretching at room-temperature compression molded specimens of low stereoregularity[2,3,9] or in mixture with form I for high stereoregular specimens. More recently Zhang et al.[10] reported the epitaxial crystallization, at low temperature, of a thin layer of sPP in form II on 2-quinoxalinol and Rastogi et al.[11] showed that form II can be obtained on cooling the isotropic melt at high pressures. Guadagno et al. described the development of form II by annealing relaxed fibers of sPP[12] or by solvent induced crystallization of unoriented samples initially in the trans-planar conformation.[13,14] Regarding the pressure and stress behavior, sPP is similar to polyethylene (PE). The latter can be obtained in the hexagonal modification crystallizing the melt at high pressures (∼0.3−0.4 GPa) or under stress at atmospheric pressure.[15,16] The main result of this paper regards the crystallization of sPP in form II, which is favored in oriented samples, where the pseudohexagonal packing in precrystalline entities favors, if preserved during crystallization, adoption of isochiral helical conformations.

The trans-planar form III is a metastable polymorph of sPP that is also characterized by an orthorhombic lattice.[5] Recently the spontaneous crystallization of an unoriented trans-planar form was obtained by quench-

* Author correspondence. Fax: +39 089 964057. E-mail: lguadagno@unisa.it.

10.1021/ma050397x CCC: $30.25
Published on Web 09/17/2005

ing sPP samples from the melt to a 0 °C bath and keeping the specimen at that temperature for a long time.[17−19] This form was interpreted either as the crystalline form III[17] or as a mesophase showing disorder in the packing of the trans-planar chains.[18] It was successively reported that this mesophase can be described assuming an orthohexagonal unit cell with parameters $a = 6.02$ Å, $b = 10.42$ Å, $c = 5.05$ Å.[19]

Because of the closeness of the energy of the different polymorphs a characteristic of sPP is the attitude to crystallize contemporaneously in different phases. Only in well-defined and, in a certain sense, "extreme" conditions a single crystalline polymorph is formed. For example, the ordered form I crystallizes as the pure polymorph only at high temperature, near the melting point of sPP; form III only at very high draw ratios maintaining the fiber under tension; and form II on cooling the melt at pressures higher than 1.2 kbar. A mixture of different structures is obtained under most experimental conditions, and even more so under processing conditions. Because of the different physical properties of the various polymorphs, the identification of the structures obtained in different experimental conditions is of the utmost importance. Quite relevant is also the path of phase transformations as a consequence of temperature and strain treatments or due to interaction with different vapor or liquid substances.

A number of different studies reported possible phase transitions paths in the complex polymorphism of sPP, but a unified view is not yet available, specifically as far as the crystallization of sPP in the helical form II is concerned. We suggested that the trans-planar mesophase could play a relevant role in the nucleation and growth of form II, by studying oriented samples which were either annealed or exposed to interacting solvents. Our data suggest that the oriented orthohexagonal mesophase, obtained by monoaxial drawing, is the precursor for crystallization of the chiral form II. The effects of the drawing, on the formation of an organized noncrystalline phase (mesophase) acting as nucleation sites for subsequent crystallization, have been already described for many polymers.[20−27] A case in point regards poly(trimethylene terephthalate) (PTT) fibers. Wu, Schultz, and co-workers demonstrated, through WAXD, SAXS, and optical birefringence experiments on partially oriented yarns of PTT prepared at different take-up speeds, that the mesophase is precursory to the crystalline phase and is depleted by the formation of the crystalline phase during spin-line stress-induced crystallization.[28,29]

In this work, we present a structural analysis of samples of sPP drawn at different temperatures. It is well documented that, after drawing at room temperature and releasing the applied tension, a large shrinkage is observed, with substantial structural changes. In the present study, new results were obtained on the transformations between the different polymorphs. Therefore, we are able to better clarify the role of the metastable trans-planar mesophase in phase transformations of sPP, specifically involving the helical form II.

Experimental Section

Syndiotactic polypropylene (sPP pellets) was bought from Aldrich Polymer Products. The polymer density, molecular weight, and melt index were respectively 0,900 g/mL, 127000, and 4.5 g/10 min (ASTM 1238).

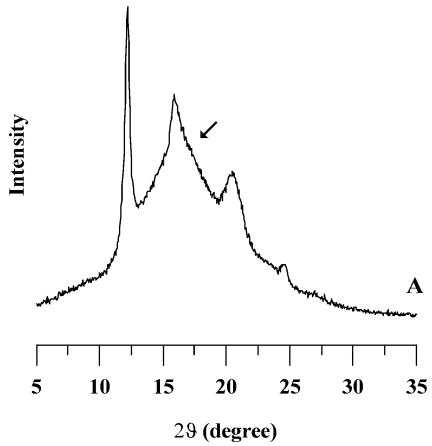

Figure 1. X-ray diffractogram of A sample.

The polymer was analyzed by ^{13}C NMR spectroscopy at 120 °C on a Bruker AM 250 spectrometer operating in the FT mode at 62.89 MHz, by dissolving 30 mg of sample in 0.5 mL of $C_2D_2Cl_4$. Hexamethyldisiloxane was used as an internal chemical shift reference. Our sample showed 89% syndiotactic pentads.

sPP pellets were molded in a hot press (Carver Inc.), at 170 °C, forming a 70 ± 5 μm thick film, which was rapidly quenched in a bath at room temperature (sample A).

Sample A was drawn at 25, 60, and 90 °C up to $\lambda = 6$ (fibers F25T, F60T, and F90T) using a dynamometric apparatus INSTRON 4310. The deformation rate was 10 mm/min, and the initial length of the sample was 10 mm. The drawn samples were analyzed by X-ray diffraction and FTIR spectroscopy under tension before unhooking. After 24 h, they were unhooked (fibers F25R, F60R, and F90R) and again analyzed.

Fiber diffraction spectra were all recorded at room temperature, under vacuum, by means of a cylindrical camera with a radius of 57.3 mm and the X-ray beam direction perpendicular to the fiber axis (Ni-filtered Cu Kα radiation). A Fuji BAS-1800 imaging plate system was used to record the diffraction patterns.

Wide-angle X-ray patterns (WAXD) were obtained using a Philips PW 1710 powder diffractometer (Cu Kα Ni-filtered radiation) with a scan rate of 2°(θ)/min.

The infrared spectra were obtained in absorbance mode using a Bruker IFS66 FTIR spectrophotometer with a 2 cm^{-1} resolution (64 scans collected).

Dynamic-mechanical properties were characterized using a Rheometrics dynamic mechanical thermal analyzer. Spectra were recorded in the tensile mode, obtaining the loss factor, tan δ, at a frequency of 1 Hz, as a function of temperature. The heating rate was 3 °C/min in the temperature range of −60 to +160 °C.

Results

Structure of the Initial Sample. In Figure 1, we show the X-ray diffraction pattern of sample A before drawing. It indicates that the sample crystallized in the usual helical form I, characterized by the most intense peaks at 12.3°, corresponding to the (200) reflection, 15.9° corresponding to the (010) reflection, and $2\vartheta = 20.8°$, corresponding to the (210−121) reflections. The absence of the (211) reflection at $2\vartheta = 18.9°$ indicates that we obtained the disordered modification of form I,

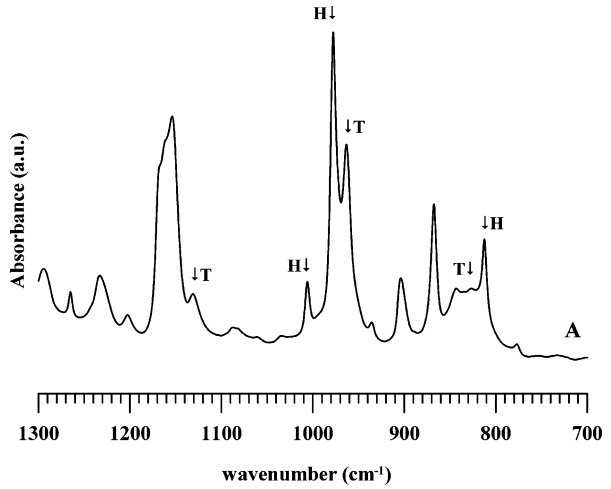

Figure 2. FT/IR spectrum in absorbance (700−1300 cm^{-1}) of A sample in which the arrows indicate the helical (H) and the trans-planar (T) peaks.

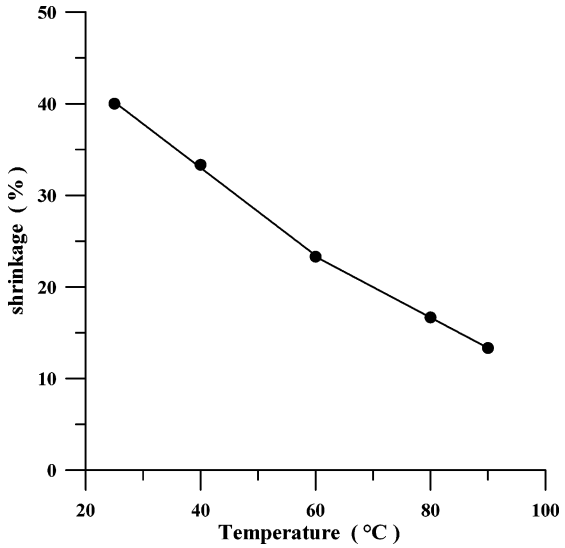

Figure 3. Shrinkage of the samples as a function of the drawing temperature.

as expected for samples crystallized at low temperatures. In fact, the preferential crystallization of the disordered form was always found in samples of low syndiotacticity or in powder samples crystallized from the melt at temperatures lower than 120 °C.[2,30,31] In this case, as is well documented in other cases, departures from the fully antichiral packing both along a and b axes may occur, leading to a less ordered form. As matter of a fact all the peaks of sample A are broad and the peak at $2\vartheta = 15.9°$ is not symmetric, showing a shoulder at $2\vartheta = 17.0°$ (see the arrow), typical of the trans-planar mesophase.[18] It was previously shown that the trans-planar mesophase can be formed keeping the sample for a long time at 0 °C, and it is stable up to 60 °C;[12,15] the present result shows that it can be formed, although in a small proportion also at 25 °C. Using the diffraction pattern of amorphous polypropylene as reference, we derived an approximate value of crystallinity by comparing the area of the crystalline peaks with the total area, that is $\alpha_c = A_c/(A_c + A_a)$, as reported in the literature.[32] The estimated value of the crystallinity α_c was 21%.

To confirm that sample A contains a fraction of chains in the trans-planar conformation we present in Figure 2 the infrared absorbance spectrum (700−1300 cm^{-1}). Infrared analysis is a very sensitive tool for the determination of chain conformation: characteristic helical and trans-planar bands have been evidenced since the first preparation of the syndiotactic isomer of polypropylene.[3,33]

Sample A shows all the helical bands, appearing at 812, 868, 977, and 1005 cm^{-1}: they are very intense and well developed. However also the trans-planar bands at 831, 963, 1132 cm^{-1} are present, although of reduced intensity as compared to the helical bands, indicating that a small fraction of chains in trans-planar conformation is also present in the sample.

Therefore, quenching the sPP melt at 25 °C allows the prevalent crystallization of form I with the chains in helical conformation but a small fraction of mesophase with the chains in trans-planar conformation also develops.

Structure of the Oriented Samples. Sample A was drawn at 25, 60, and 90 °C up to $\lambda = 6$ and left 24 h under tension at room temperature. When the fibers were unhooked, they underwent a large shrinkage, depending on the drawing temperature. The shrinkage is shown as a function of the drawing temperature in Figure 3 It is expressed as $(l_{max} - l_f)/l_{max}$, where l_{max} is the length at full extension before relaxation and l_f is the length after releasing the tension. We can observe that the percentage of shrinkage is very large at room temperature and almost linearly decreases on increasing the drawing temperature, being 40% for the sample drawn at 25 °C and 13% for the sample drawn at 90 °C. The values of the shrinkage are always much larger than those (2−3%) observed in most semicrystalline polymers drawn in different conditions.

The crystalline phase composition was investigated in both the fixed and relaxed fibers. In Figure 4, we show the X-ray fiber diffraction patterns of the fixed (F25T, F60T, and F90T) and relaxed fibers (F25R, F60R, and F90R). Relevant observed reflections, spacings, the corresponding 2θ (deg) values, and indices for helical and trans-planar forms are listed in Table 1. The indices of the reflections of form I are given both for the traditional unit cell with $b = 5.60$ Å (form I^a) and for the unit cell with doubled b (form I^b).

Fiber Oriented at 25 °C. Elongation of the sample at 25 °C determines the transformation of the helical form I into the trans-planar form III, with a high orientation as long as the sample is under tension. On the equator we observe two intense reflections at $2\vartheta = 15.87°$ (020 of form III) and $2\vartheta = 18.76°$ (110 of form III), and a less intense reflection at $2\vartheta = 29.47°$, indexed as 130 of form III. The first two intense reflections are superimposed with the reflection at $2\vartheta = 17.0°$, which may pertain either to the helical form II or to the trans-planar mesophase. On the trans-planar phase layer, with identity period of 5.05 Å, an intense reflection at $2\vartheta = 23.73°$ is apparent. A very weak reflection is also observed at $2\vartheta = 20.86°$, on the layer with periodicity 7.45 Å, typical of all the helical forms.

Considering that the intensity of the reflection at $2\vartheta = 17.0°$ is very high as compared to the reflection of the helical first layer, we must associate this reflection to the trans-planar mesophase, even if the presence of a small fraction of form II cannot be excluded. On the other hand, as well documented in the literature, drawing at room-temperature always produces the

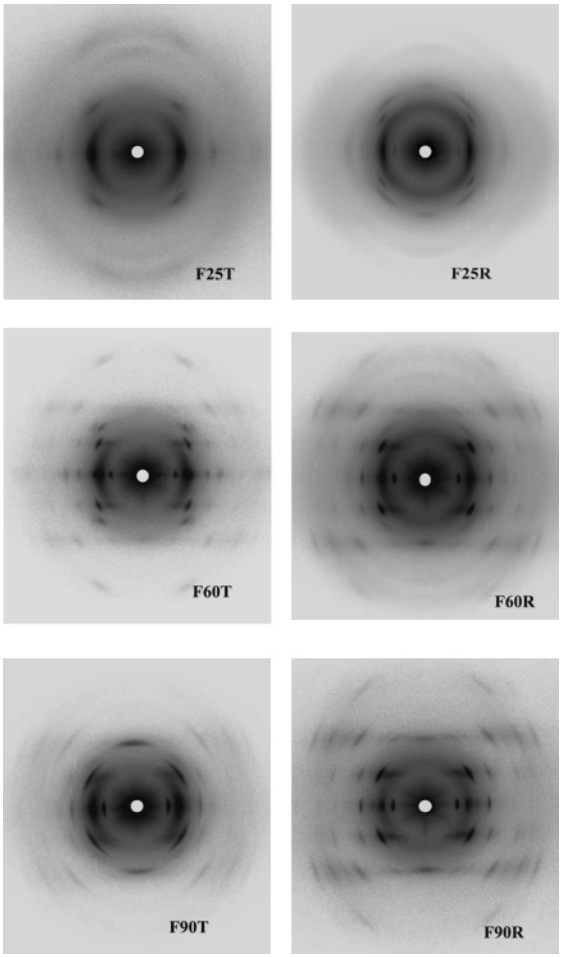

Figure 4. X-ray diffraction patterns of fibers before (F25T, F60T, F90T) and after releasing the tension (F25R, F60R, F90R).

trans-planar mesophase, unless very high draw ratios are attained.

In the pattern of the relaxed fiber F25R, we observe the intensification of the reflection at $2\vartheta = 12.32°$, observed in all helical modifications, the presence of a reflection at $2\vartheta = 17.0°$ and a weak reflection at $2\vartheta = 29.70°$. On the layer with identity period 7.45 Å, the reflection at $2\vartheta = 20.86°$ is apparent, whereas on the layer with identity period 5.05 Å we observe the reflection of the trans-planar mesophase at $2\vartheta = 23.73°$. Comparing the diffraction pattern of the fiber under tension and of the released fiber we note the following points:

(a) The amorphous fraction is much less oriented in the relaxed fiber.

(b) In the relaxed fiber the reflections of the crystalline form III, both on the equator (15.9° and 18.8° of 2ϑ) and on the first layer (29.47° of 2ϑ) are absent, whereas the first layer reflection of the trans-planar mesophase is still present.

(c) The intensity of the reflection at $2\vartheta = 17.0°$ is considerably increased in the relaxed sample, resulting the most intense of the pattern. Indeed it pertains to both the trans-planar mesophase and the helical form II.

(d) The helical form present in the relaxed sample is form II, as shown by the presence of the reflections at $2\vartheta = 17.0°$ (indexed as 110 of form II) on the equator, and at $2\vartheta = 20.86°$ (indexed as 111) on the first layer. This attribution is confirmed by the absence on the equator of the reflection at $2\vartheta = 16.02°$, typical of form I.

In conclusion, in the fixed fiber we observe the coexistence of the crystalline form III and the trans-planar mesophase with a very small fraction of a helical form, whereas in the relaxed fiber we observe the disappearance of form III and the clear presence of the helical form II together with the trans-planar mesophase.

Fiber Oriented at 60 °C. The pattern of the fixed fiber F60T, drawn at 60 °C, shows both high orientation and crystallinity. On the equator we can identify the reflection at $2\vartheta = 12.32°$ (indexed as 200 for all the helical forms) and four partially superimposed reflections: at $2\vartheta = 15.9°$ (indexed as 020 of form III), at $2\vartheta = 16.02°$ (indexed as 010 for form I), at $2\vartheta = 17.0°$ (distinctive of both the trans-planar mesophase and the helical form II), and at $2\vartheta = 18.76°$ (form III). Moreover, we observe the reflections at $2\vartheta = 24.79°$ (indexed as 400 for all the helical forms) and $2\vartheta = 29.47°$ (indexed as 130 for form III).

On the layer with identity period 7.45 Å, the reflections at $2\vartheta = 17.44°$ (indexed as 201 for both form I and form II), $2\vartheta = 20.86°$ and 27.38°, both typical of all of the helical forms, are present. On the layer with an identity period of 5.05 Å, the reflections 021 and 111 of form III described by Chatani[5] are apparent.

From the described data we can infer the presence in the fiber drawn at 60 °C and kept under tension, of crystals of both the disordered helical forms I and II. Also form III crystals and the mesophase domains with chains in trans-planar conformation are evidenced, although in a smaller proportion. Fiber F60T is a very interesting case of coexistence under tension of polymorphs with chains in different conformation, both helical and trans-planar.

In the relaxed F60R fiber, we observe that all the distinctive reflections of form III on the equator disappeared, whereas the intensity of the equatorial peak at $2\vartheta = 17.0°$ increased. On the layer with 5.05 Å periodicity, we observe only the reflection at $2\vartheta = 23.73°$. This reflection, together with the peak at $2\vartheta = 17.0°$ on the equator, is distinctive of the trans-planar mesophase. However we can observe that the intensity of the equatorial reflection at $2\vartheta = 17.0°$ is too high, as compared to the trans-planar reflection on the first layer, and therefore we must assume a contribution to this equatorial peak of the helical form II since the equatorial peak at $2\vartheta = 17.0°$ is distinctive of both the helical form II and the trans-planar mesophase. Summarizing, in the relaxed fiber F60R, both forms I and II crystals with chains in the helical conformation, coexist with trans-planar mesophase.

Fiber oriented at 90 °C. With considerations closely similar to those put forward relative to fiber F60T, we can deduce that the ordered domains of sample F90T are formed by a mixture of crystals of both the disordered form I, form II and of a fraction of trans-planar mesophase. Fiber F90T is less oriented than fiber F60T, due to the high drawing temperature, near to the crystalline melting point of sample A (about 130 °C) which allows considerable relaxation. When the tension on the fiber is released, both the crystallinity and the orientation increase in the F90R fiber. In the following section, an increase of crystallinity in the relaxed fiber with respect to the fixed fiber, due to the transformation

Table 1: Reflections Observed in the X-ray Diffraction Spectra of Stretched and Relaxed Samples

sample	period along chain axis (Å)	2θ, deg (Cu)	distance (Å)	I	*hkl*[c]
F25T (fiber $\lambda = 6$)		15.87	5.58	vs	020 form III
		17.00	5.21	ms	trans-planar mesophase
					110 form II
		18.76	4.73	vs	110 form III
		29.47	3.03	mw	130 form III
	7.45	20.86	4.26	vvw	111 form I,[a] form II
					121 form I[b]
	5.05	23.7 3	3.75	s	021 form III
					trans-planar mesophase
F25R (fiber $\lambda = 3.6$)		12.32	7.18	ms	200 form I,[a]form I,[b] form II
		17.00	5.21	vs	trans-planar mesophase
					110 form II
		29.70	3.00	vw	trans-planar mesophase
	7.45	20.86	4.26	ms	111 form I,[a] form II
					121 form I[b]
	5.05	23.7 3	3.75	ms	021 form III
					trans-planar mesophase
F60T (fiber $\lambda = 6$)		12.32	7.18	s	200 form I,[a] form I,[b] form II
		15.87	5.58	s	020 form III
		16.02	5.53	s	020 form I[b]
					010 form I[a]
		17.00	5.21	ms	trans-planar mesophase
					110 form II
		18.76	4.73	s	110 form III
		24.79	3.59	mw	400 form I,[a] form I,[b] form II
		29.47	3.03	w	130 form III
	7.45	17.44	5.09	vw	201 form I,[a] form II
		20.86	4.26	vs	111 form I,[a] form II
					121 form I[b]
		27.38	3.26	w	311 form I,[a] form II
					321 form I[b]
					401 form I,[a] form II
	5.05	23.73	3.75	ms	021 form III
					trans-planar mesophase
		25.78	3.46	w	111 form III
F60R (fiber $\lambda = 4.6$)		12.32	7.18	s	200 form I,[a]form I,[b] form II
		16.02	5.53	s	020 form I[b]
					010 form I[a]
		17.00	5.21	s	trans-planar mesophase
					110 form II
		24.79	3.59	ms	400 form I,[a] form I,[b] form II
	7.45	17.44	5.09	ms	201 form I,[a] form II
		20.86	4.26	vs	111 form I,[a] form II
					121 form I[b]
		27.38	3.26	vw	311 form I,[a] form II
					321 form I[b]
					401 form I,[a] form II
	5.05	23.7 3	3.75	ms	trans-planar mesophase
F90T (fiber$\lambda = 6$)		12.32	7.18	vs	200 form I,[a] form I,[b] form II
		16.02	5.53	s	020 form I[b]
					010 form I[a]
		17.00	5.21	s	trans-planar mesophase
					110 form II
		24.79	3.59	ms	400 form I,[a] form I,[b] form II
	7.45	17.44	5.09	vw	201 form I,[a] form II
		20.86	4.26	s	111 form I,[a] form II
					121 form I[b]
		27.38	3.26	vw	311 form I,[a] form II
					321 form I[b]
					401 form I,[a] form II
	5.05	23.73	3.75	vw	trans-planar mesophase
F90R (fiber $\lambda = 5.2$)		12.32	7.18	ms	200 form I,[a] form I,[b] form II
		16.02	5.53	vs	020 form I[b]
					010 form I[a]
		17.00	5.21	vs	110 form II
		20.06	4.43	mw	220 form I[a]
					210 form I[b]
		24.79	3.59	vs	400 form I,[a]form I,[b] form II
	7.45	17.44	5.09	s	201 form I,[a] form II
		18.84	4.71	ms	211 form I[b]
		20.86	4.26	vs	111 form I,[a] form II
					121 form I[b]
		27.38	3.26	w	311 form I,[a] form II
					321 form I[b]
					401 form I,[a] form II

[a] Form I orthorhombic unit cell with axes $a = 14.5$ Å, $b = 5.6$ Å, and $c = 7.45$Å. [b] Form I orthorhombic unit cell with axes $a = 14.5$ Å, $b = 11.2$ Å, and $c = 7.45$Å. [c] Crystalline forms where the reflection is allowed.

of the trans-planar mesophase, will be shown. The interesting and unexpected morphological change related to the orientation increase, will be investigated in a forthcoming paper (manuscript in preparation). We can anticipate that the effect is probably related to the conformational transition from the trans-planar to the $(T_2G_2)_2$ helical conformation in both the amorphous, mesomorphic and the crystalline components of the sample. As for the crystalline forms present in the relaxed sample we observe that there are no more reflections on the layer corresponding to a fiber repeat of 5.05 Å. Therefore, the equatorial reflection at $2\vartheta = 17.0°$ must be assigned to the helical form II. Indeed this reflection is very sharp and shows an azimuthal spread comparable to the other helical reflections. This is normally not the case when the trans-planar mesophase is present. In conclusion, drawing at 90 °C does not allow the formation of the trans-planar crystalline form III but only of the trans-planar mesophase, whereas in the relaxed fiber there is the coexistence of all the helical forms and the disappearance of ordered domains in trans-planar conformation indicating that the trans-planar mesophase relaxes to a helical form.

Overall Crystallinity Index of the Fibers from WAXD. The analysis of the phase composition of the fibers from the 2D WAXD patterns in Figure 4 was performed using procedures similar to others previously shown in the literature.[34−36] All of these procedures allow one to obtain the crystallinity index from imaging plate gray scale images by the analysis of the diffracted intensity integrated azimuthally from 0 to 360°.

In the present case, this procedure was applied in the 2θ range where significant scattering takes place (8.0−40.0°). The diffracted intensity was integrated azimuthally from 0 to 360° for all diffraction angles in the select range of 2θ. The data were averaged along the azimuthal angle β using the following equation:

$$\bar{I}(2\vartheta) = \frac{1}{2\pi}\int_0^{2\pi} I(2\vartheta,\beta)\, \mathrm{d}\beta$$

Then a deconvolution into crystalline diffraction peaks and an amorphous halo was done.

The index related to a generic phase (α_{phase}) is obtained applying the following equation:

$$\alpha_{phase} = \frac{\int_{2\vartheta_1}^{2\vartheta_2} \bar{I}_{phase}(2\vartheta)\, \mathrm{d}(2\vartheta)}{\int_{2\vartheta_1}^{2\vartheta_2} \bar{I}_{overall}(2\vartheta)\, \mathrm{d}(2\vartheta)}$$

Here $[2\vartheta_1,2\vartheta_2]$ integral boundaries are the angles abovementioned and *overall* is related to the overall scattering signal (amorphous phase, all the possible crystalline forms and the trans-planar mesophase if present).

According to the previous equation, the crystallinity index was defined as follows:

$$\alpha o = \frac{\int_{2\vartheta_1}^{2\vartheta_2} \bar{I}_{(c+m)}(2\vartheta)\, \mathrm{d}(2\vartheta)}{\int_{2\vartheta_1}^{2\vartheta_2} \bar{I}_{overall}(2\vartheta)\, \mathrm{d}(2\vartheta)}$$

where $\bar{I}_{(c+m)}$ takes account of the crystalline phase and the eventual trans-planar mesophase. The authors would like to emphasize the mean of the crystallinity index α_o. This index is related to the overall contribute of the organized phases which includes in addition to all the possible crystalline forms the trans-planar mesophase.

Table 2: Amorphous Index (α_a) and Crystallinity Index (α_o = Crystalline Phase and Trans-Planar Mesophase) in Fixed and Relaxed Fibers[a]

fixed fibers	α_a (%)	α_o (%)	relaxed fibers	α_a (%)	α_o (%)
F25T	61 ± 3	39 ± 2	F25R	68 ± 3	32 ± 2
F60T	68 ± 3	32 ± 2	F60R	69 ± 3	31 ± 2
F90T	66 ± 3	34 ± 2	F90R	63 ± 3	37 ± 2

[a] Estimated error bars are supplied.

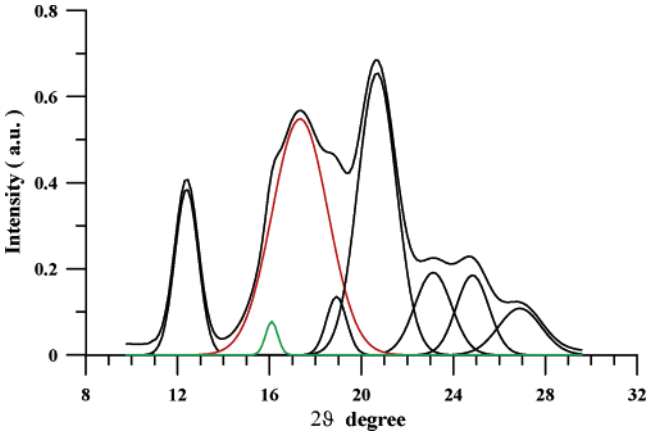

Figure 5. Intensity of azimuthal integrated signals with the related fittings vs Bragg angle for the crystalline component of F90R fiber.

Table 2 shows the crystallinity α_o and amorphous α_a indexes for all the analyzed fibers. The errors related to the peaks deconvolution are estimated by calculating the percentage of the residuals after the peaks deconvolution process.

Data in Table 2 show that, in the limit of the experimental error, the amorphous phase index is substantially unchanged when the applied stress is released. This result highlights that the strong structural changes observed in Figure 4 following the relaxation of the fibers must be attribute to the organized phase, which does not vary in the overall percentage phase but in the phase composition of its components. For example, α_o (%) is 34 ± 2 and 37 ± 2 in the fixed (F90T) and relaxed fibers (F90R), respectively. While the F90R fiber contains only crystalline domains with chains in helical conformation, the most ordered phase in the F90T fiber also contains domains with chains in trans-planar conformation.

It is evident that the trans-planar mesophase transforms into domains with chains in helical conformation in the relaxed fiber where the crystallinity index does not change.

Unfortunately the complex polymorphism of the organized phase in our systems does not allow the application of a rigorous quantitative analysis of the ordered components.

To give an idea of this complexity, we show in Figure 5, for the F90R fiber, the deconvolution of the scattered intensity of the ordered phase into crystalline diffraction peaks.

A peak of reduced intensity at $2\theta = 16°$ (form I, green trace), and a very intense peak $2\theta = 17°$ (form II, red trace) are observed. These results confirm the large percentage of form II in the fiber. A rigorous calculation

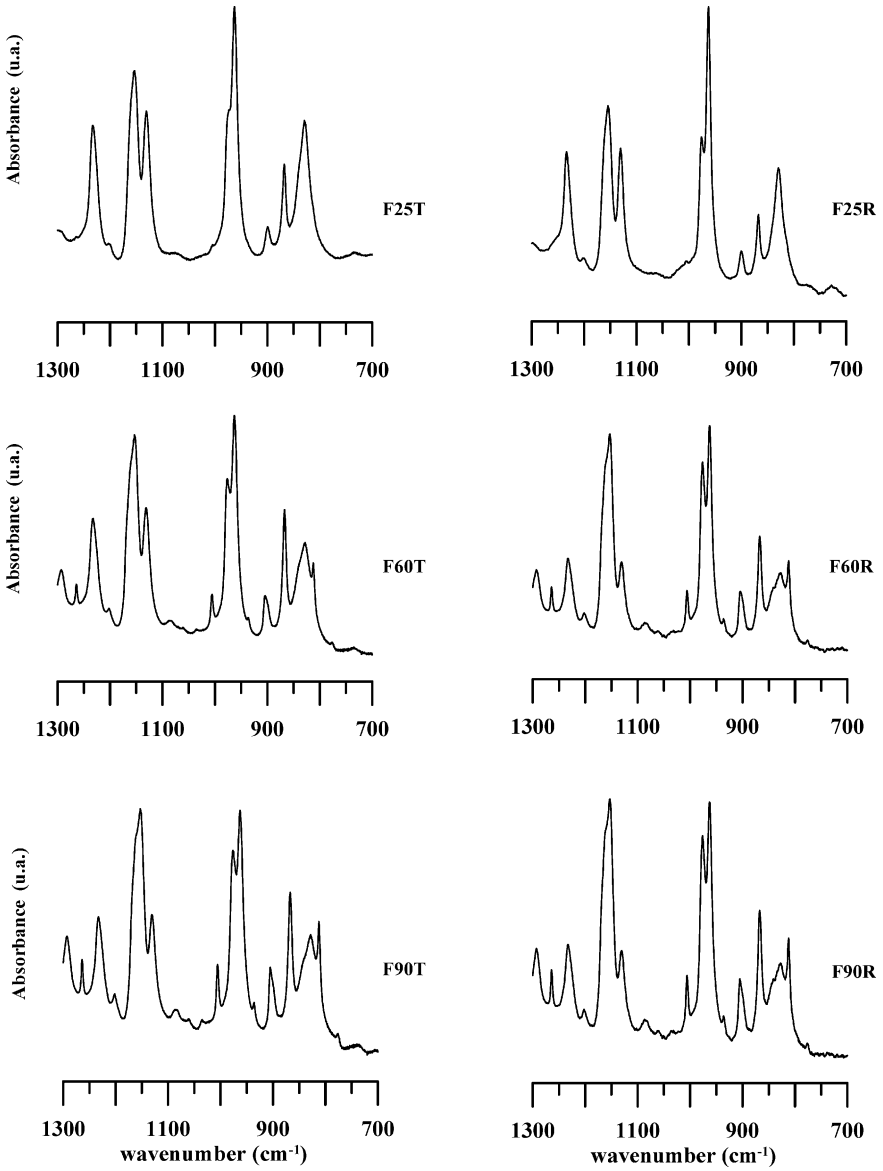

Figure 6. FT/IR spectra in absorbance (700−1300 cm^{-1}) of fibers before (F25T, F60T, F90T) and after releasing the tension (F25R, F60R, F90R).

of form II percentage requires not only the knowledge of the area at $2\theta = 17°$ peak but also the evaluation of the fraction of the area related to this component in the other peaks. In fact, the area of peak at $2\theta = 12.3°$ is due to both the crystalline contributes of form I and form II.

The issue of the repartition of the area between different crystalline forms regards also other peaks (for example at $2\theta = 20.8°$) and a repartition of single peaks in different components seems to us a very forced elaboration. This situation is even more complex for fibers containing the trans-planar mesophase whose reflection at $2\theta = 17°$ superimposes on the peak of form II.

For this reason, we accept as quantitative datum only the overall crystallinity index (as above defined). This analysis, although limited in the obtained information, provides us a useful tool for understanding the phases involved in the phase transformations during the relaxation of the fibers. However in this paper the results of this analysis are also supported by dynamic−mechanical analysis which allows a semiquantitative evaluation of the components of the organized phase.

Infrared Analysis. In Figure 6, we report the FTIR spectra in absorbance (700−1300 cm^{-1}) of the fibers under tension (F25T, F60T and F90T) and after releasing the tension (F25R, F60R, and F90R). The infrared analysis can help one better understanding the structural organization, by observing the conformational changes in the fibers oriented at increasing temperatures, before and after releasing the tension.

Sample F25T shows very intense and sharp trans-planar bands. The helical conformations bands are absent (as the band at 812 cm^{-1}) or very much reduced. The band at 977 cm^{-1}, assigned to helical chains also in the amorphous phase[19,37,38] appears just as a shoulder of the very intense peak at 963 cm^{-1}, typical of the trans-planar conformations. Increasing the drawing temperature, we observe in the fixed fibers the appearance or the increase of the helical bands (e.g., at 812 and 1005 cm^{-1}). Upon releasing the tension we observe in fiber F25R only an increase of the band at 977 cm^{-1}, whereas the band at 812 cm^{-1}, attributed to form I,[37,38] is absent, confirming the results of the X-ray analysis. The relaxed fibers F60R and F90R show an increase in the helical bands and a correspondent decrease of the

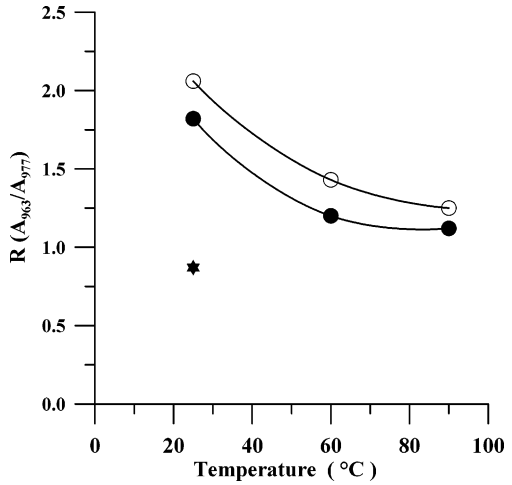

Figure 7. Absorbance ratio [$A_{963\ cm^{-1}}/A_{977\ cm^{-1}}$] as a function of the drawing temperature: (○) fixed fibers; (●) relaxed fibers and (★) A sample.

trans-planar bands. A parameter commonly used to measure the overall relative planar-to-helical content of sPP is the A ($_{963\ cm^{-1}}$)/A ($_{977\ cm^{-1}}$) absorbance ratio. The value of this parameter as a function of the drawing temperature is reported in Figure 7 for both the fixed and the relaxed fibers. For either series a steep decrease of the proportion of trans-planar to helical chain conformation is observable between 25 and 60 °C, whereas a smoother decrease occurs for higher temperatures. Interestingly, if compared to the value detected in the original sample before drawing (A), the trans-planar chain conformation content is always very high, even in fiber F90R for which X-ray analysis did not show any trans-planar presence in the ordered phases. It should be recalled that the infrared band at 977 cm^{-1} represents the helical chain conformation also in the amorphous phase, and the 963 cm^{-1} the trans-planar conformation both in the amorphous and in the mesophase. Moreover the helical form II usually is accompanied by strands in trans-planar conformation reported as "kink bands"[39] and therefore the presence of trans-planar bands is an expected result in the infrared spectrum of samples in form II, even in the absence of any ordered trans-planar phase. Indeed, the infrared spectrum of fiber F90R suggests that form II is the prevalent crystalline form in the relaxed fiber.

Dynamic Mechanical Analysis of the Relaxed Fibers. In previous papers,[13,40,41] we have analyzed the structure and the dynamic-mechanical behavior of different sPP polymorphs. We have correlated the thermal transitions of the different sPP polymorphs with the tan δ dissipation peaks observed in the dynamic mechanical analysis, and have found that each dissipation peak is distinctive of a particular polymorph. The helical form I shows only the transition of the amorphous phase, related to the glass transition, appearing at about 20 °C. The trans-planar mesophase shows, besides the amorphous glass transition, a dissipation peak centered at 70 °C, due to the transition of the trans-planar chains into the helical conformation. The helical form II shows an intense tan δ peak at ca. 120 °C. This peak was associated with the melting of form II and recrystallization into the more stable helical form I.[13,40] The summarized results make the dynamic-mechanical analysis an effective tool to recognize the presence of the different sPP polymorphs, also in cases in which X-ray analysis is not able to discriminate, for example when we obtain the coexistence of the trans-planar mesophase and the helical form II, which share the same distinctive peak at $2\vartheta = 17.0°$.

The relaxed fibers were analyzed with a dynamic-mechanical strain and the tan δ dissipation curves, obtained between −60 and +180 °C, are reported in Figure 8, for samples F25R, F60R, and F90R. Fiber F25R shows three peaks, at 20, 70, and 120 °C that can be associated with the presence of the amorphous phase, the trans-planar mesophase and form II, respectively. The relaxed fiber F60R, besides the amorphous peak, shows a broad not symmetric peak centered at 120 °C, associated with the presence of form II. Between the two peaks a broad transition due to the trans-planar mesophase can be detected, indicating however that the fraction of mesophase is not very high. Fiber F90R shows the peak of the amorphous phase at 20 °C and a very well separated and sharp peak due to the helical form II. The high intensity of the form II peak indicates that a large fraction of the helical phase crystallized in this form. In conclusion, dynamic-mechanical analysis indicates that, increasing the drawing temperature, the mesophase present in the fixed fibers increasingly transforms into the helical form II. It is present in a relevant fraction in sample F25R, relaxed from a fiber in which form III was present.

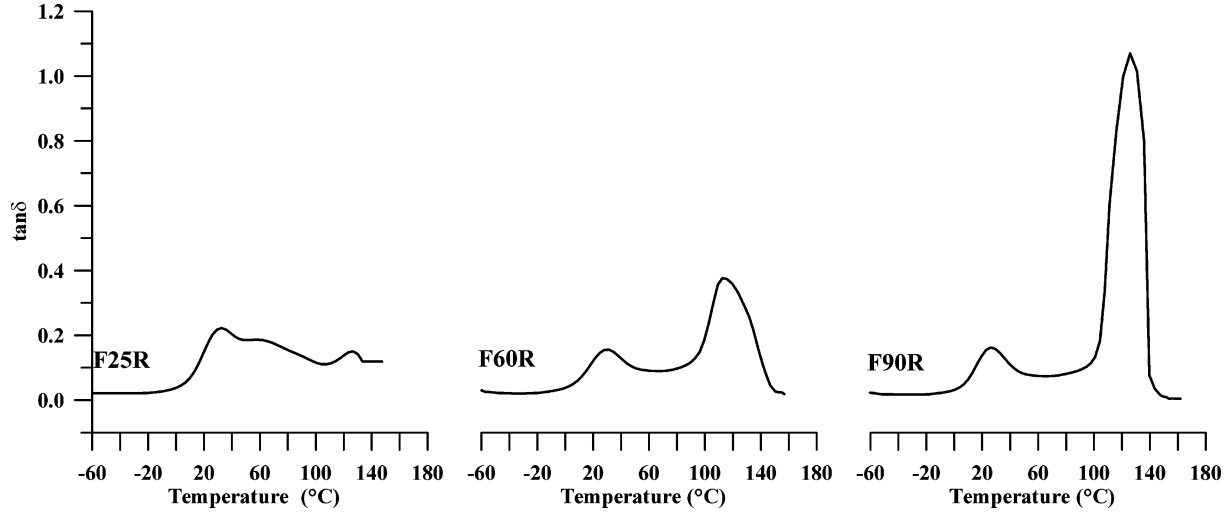

Figure 8. Dissipative factor (tan δ) as a function of temperature for F25R, F60R, and F90R samples.

Concluding Remarks

The experimental observations we presented confirm that the trans-planar mesophase does play a significant role in the crystallization of sPP in form II. We have previously reported that annealing at 80 °C unoriented samples containing the trans-planar mesophase leads to crystallization into form II. In the present paper, we investigated the relaxation behavior of fibers that contain significant amounts of the trans-planar mesophase. Also in the present case, i.e., in the relaxation behavior, we found that the presence of the trans-planar mesophase or of some amount of form II in the fixed fiber is a prerequisite for further crystallization into form II to occur.

Form II is a peculiar, metastable crystalline modification of sPP. Packing energy calculations and thermal data indicate that at ambient pressure it is less stable than form I, although the two modifications share the same $(T_2G_2)_n$ conformation and have closely comparable density. Another feature of form II is that, even if the sPP chain is nonchiral, it adopts a chiral space group and hence individual crystals are built of helices sharing the same chirality. A chiral crystal structure for a nonchiral system as sPP, seems less probable than a packing where an equal number of left- and right-handed helices coexist, like the one found in the more stable form I. Thus, crystallization into form II rather than form I is likely to be caused, under appropriate conditions, by a greater growth rate or by preferential nucleation.

The outlined crystallization behavior of form II appears consistent with the proposal put forward by Allegra et al.[42] that pseudohexagonal packing in precrystalline states as found in the trans-planar mesophase of sPP, favors, if preserved during crystallization, adoption of isochiral helical conformations in crystals of nontrivial helical molecules. Indeed, according to the mentioned paper, the degree, expressed by the hexagonality index H, to which a crystal structure of nontrivially helical molecules approach pseudohexagonal packing is strongly correlated to the probability of the crystal structure being chiral. The hexagonality index H, which is 1.00 for hexagonal structures, is found to be 1.39 for the chiral form II and 1.64 for the achiral form I.

It is interesting to note that in sPP the trans-planar conformation, accessed essentially in strained samples, favors crystallization with a pseudohexagonal packing (in the mesophase) or very close to pseudohexagonal in the case of form III. In turn such pseudohexagonal arrangements, to be expected to some degree also locally in oriented amorphous sPP, are likely to favor upon further evolution into helical polymorphs, the crystallization into the chiral form II rather than into the racemic form I. This would explain the higher propensity of oriented samples to yield form II as compared to crystallization from the melt into unoriented bulk samples or solution grown crystals.

Form II develops also releasing the stress: the trans conformation under the described circumstances appears to evolve into the more stable $(T_2G_2)_2$ conformation rapidly enough to maintain some memory of the pseudohexagonal chain packing, of which form II is reminiscent.

The process is not likely to occur directly from the ordered form III to form II but to develop through the partial disordering of the lower density trans-planar mesophase. We are led to confirm the central role we already proposed for the trans-planar mesophase, modified as shown in Scheme 1.

Scheme 1. Summary of Phase Transitions for Stereoregular SPP at Ambient Pressure

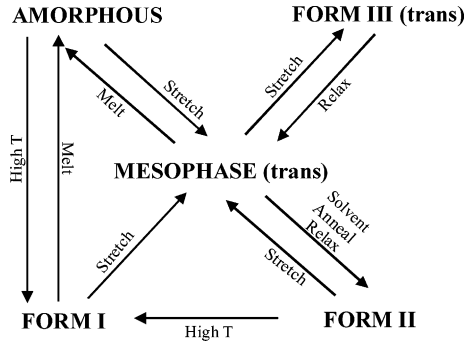

Direct transitions between the amorphous phase and form III, form II and form IV seem particularly unlikely; while direct form II−form I transitions are basically impossible. The role of the metastable trans-planar mesophase may well be quite central in the crystallization of different polymorphs of sPP.

We can safely state that in none of our samples where the crystalline trans-planar form III is present, crystallization into form II occurs, unless also the trans-planar mesophase or some amounts of form II are already present. Form II under appropriate conditions will evidently also be able to lead to self-nucleation.

The $(T_6G_2T_2G_2)_n$ conformation found in form IV could represent in principle, an ordered ideal intermediate step between form III and form II. The three forms have all a centered cell, not far from a hexagonal packing and furthermore form IV and form II are characterized by a) chiral space groups i.e., individual crystals built of isochiral chains b) closely similar chain projection packing (lattice constants differ by ca. 2%). A deeper study of the differences between fixed and relaxed fibers obtained at high temperature, in particular the fiber drawn at 60 °C, is currently under investigation to ascertain or reject this hypothesis.

Acknowledgment. This work was supported by MIUR−Italia PRIN 2002.

References and Notes

(1) Lotz, B.; Lovinger, A. J.; Cais, R. E. *Macromolecules* **1988**, *21*, 2375.
(2) De Rosa, C.; Corradini, P. *Macromolecules* **1993**, *26*, 5711.
(3) Corradini, P.; Natta, G.; Ganis, P.; Temussi, P. A. *J. Polym. Sci.* **1967**, *16*, 2477.
(4) Uehara, H.; Yamazachi, Y.; Kanamoto, T. *Polymer* **1966**, *37*, 57.
(5) Chatani, Y.; Maruyama, H.; Noguchi, K.; Asanuma, T.; Shiomura, T. *J. Polym. Sci., Part C* **1990**, *28*, 393.
(6) Chatani, Y.; Maruyama, H.; Asanuma, T.; Shiomura, T. *J. Polym. Sci., Part B: Polym. Phys. Ed.* **1991**, *29*, 1649.
(7) Lovinger, A. J.; Lotz, B.; Cais, R. E. *Polymer* **1990**, *31*, 2253.
(8) De Rosa, C.; Auriemma, F.; Vinti, V. *Macromolecules* **1997**, *30*, 4137.
(9) De Rosa, C.; Auriemma, F.; Vinti, V. *Macromolecules* **1998**, *31*, 7430.
(10) Zhang, J.; Yang, D.; Thierry, A.; Wittmann, J. C.; Lotz, B. *Macromolecules* **2001**, *34*, 6261.
(11) Rastogi, S.; La Camera, D.; Van der Burgt, F.; Terry, A. E.; Cheng, S. Z. D. *Macromolecules* **2001**, *34*, 7730.
(12) Guadagno, L.; D'Aniello, C.; Naddeo, C.; Vittoria, V.; Meille, S. V. *Macromolecules* **2003**, *36*, 6756.
(13) Guadagno, L.; D'Aniello, C.; Naddeo, C.; Vittoria, V. *J. Macromol. Sci. Phys. B* **2004**, *43* (4), 883.

(14) Guadagno, L.; D'Aniello, C.; Naddeo, C.; Vittoria, V.; Meille, S. V. *Macromol. Symp*, **2004**, in press.
(15) Basset, D. C. The crystallization of polyethylene at high pressures. In *Developments crystalline polymers*; Applied Science Publishers: London, 1982.
(16) Rastogi, S.; Odell, J. A. *Polymer* **1993**, *34*, 1523.
(17) Nakaoki, T.; Ohira, Y.; Hayashi, H.; Horii, F. *Macromolecules* **1998**, *31*, 2705.
(18) Vittoria, V.; Guadagno, L.; Comotti, A.; Simonutti, R.; Auriemma, F.; De Rosa, C. *Macromolecules* **2000**, *33*, 6200.
(19) Guadagno, L.; D'Aniello, C.; Naddeo, C.; Vittoria, V.; Meille, S. V. *Macromolecules* **2002**, *35*, 3921.
(20) Janeschitz-Kriegl, H.; Wimberger-Friedl, R.; Krobath, G.; Liedauer, S. *Kunststoffe* **1987**, *40*, 301.
(21) Eder, G.; Janeschitz-Kriegl, H. *Colloid Polym. Sci.* **1988**, *266*, 1087.
(22) Eder, G.; Janeschitz-Kriegl, H.; Krobath, G. *Pro. Colloid Polym. Sci.* **1989**, *80*, 1.
(23) Eder, G.; Janeschitz-Kriegl, H.; Liedauer, S. *Prog. Colloid Polym. Sci.* **1990**, *15*, 629.
(24) Jerschow, P.; Janeschitz-Kriegl, H. *Int. Polym. Process.* **1997**, *12*, 72.
(25) McHugh, A. J.; Guy, R. K.; Tree, D. A. *Colloid Polym. Sci.* **1993**, *271*, 629.
(26) Bushman, A. C.; McHugh, A. J. *J. Appl. Polym. Sci.* **1997**, *64*, 2165.
(27) Kumaraswamy, G.; Issaian, A. M.; Kornfield, J. A. *Macromolecules* **1999**, *32*, 7537.
(28) Wu, J.; Schultz, J. M. *Polymer* **2002**, *43*, 6695.
(29) Wu, J.; Schultz, J. M.; Samon J. M.; Pangelinam, A. B.; Chuah, H. H. *Polymer* **2001**, *42*, 7161.
(30) Guadagno, L.; D'Aniello, C.; Naddeo, C.; Vittoria, V. *Macromolecules* **2000**, *33*, 6030.
(31) Guadagno, L.; D'Aniello, C.; Naddeo, C.; Vittoria, V. *Macromolecules* **2001**, *34*, 2521.
(32) Natta, G.; Corradini, P.; Cesari, M. R. *Acc. Lincei 1957*, s *8*, 22, 11.
(33) Natta, G.; Corradini, P.; Ganis, P. *Makromol. Chem.* **1960**, *39*, 238.
(34) Wu, J.; Schultz, J. M.; Samon J. M.; Pangelinam, A. B.; Chuah, H. H. *Polymer* **2001**, *42*, 7131.
(35) Kolb, R.; Seifert, S.; Stribeck, N.; Zachman, H. G. *Polymer* **2000**, *41*, 1497.
(36) Martorana, A.; Piccarolo, S.; Scichilone, F. *Macromol. Chem. Phys.* **1997**, *198*, 597.
(37) Sevegney, S. M.; Parthasarthy, C.; Kannan, R. M.; Thurman, D. W.; Ballester, L. F. *Macromolecules* **2003**, *36*, 6472.
(38) Guadagno, L.; D'Arienzo, L.; Vittoria, V. *Macromol. Chem. Phys.* **2000**, *201*, 246.
(39) Auriemma, F.; De Rosa, C.; Ruiz de Ballesteros, O.; Corradini, P. *Macromolecules* **1997**, *30*, 6586.
(40) Guadagno, L.; D'Aniello, C.; Naddeo, C.; Vittoria, V.; Romano, G. *J. Macromol. Sci. Phys. B* **2004**, *43* (2), 349.
(41) Gorrasi, G.; Guadagno, L.; D'Aniello, C.; Naddeo, C.; Romano, G.; Vittoria, V. *Macromol. Symp.* **2003**, *203*, 285.
(42) Meille, S. V,; Allegra, G. *Macromolecules* **1995**, *28*, 7764.

MA050397X